Dyes and Pigments 200 (2022) 110138

Contents lists available at ScienceDirect

Dyes and Pigments

journal homepage: www.elsevier.com/locate/dyepig

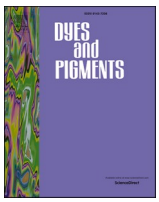

Influence of indigo-hydroxyl interactions on the properties of sepiolite-based Maya blue pigment

Li Li [a,b,c], Guanzheng Zhuang [d,*], Mengyuan Li [a,b,c], Peng Yuan [a,b], Liangliang Deng [d], Haozhe Guo [d]

[a] CAS Key Laboratory of Mineralogy and Metallogeny, Guangdong Provincial Key Laboratory of Mineral Physics and Materials, Guangzhou Institute of Geochemistry, Chinese Academy of Sciences, Guangzhou, 510640, China
[b] CAS Center for Excellence in Deep Earth Science, Guangzhou, 510640, China
[c] University of Chinese Academy of Sciences, Beijing, 100049, China
[d] Institute of Resources Utilization and Rear Earth Development, Guangdong Academy of Sciences, Guangzhou, 510650, China

ARTICLE INFO

Keywords:
Maya blue
Water molecules
Hydrogen bonds
Organic dyes
Stability

ABSTRACT

Maya blue is a greenish-blue and stable pigment composed of indigo and palygorskite or sepiolite. Previous studies implied that the properties of Maya blue were influenced by different hydroxyl groups in the clay structure, e.g., zeolitic water, coordinated water, and structural hydroxyls. Therefore, an in-depth investigation was planned to analyze the structures and properties of indigo-sepiolite hybrid pigments in this work. Sepiolite materials were heated at 160, 360, 610, and 880 °C to remove zeolitic water, the first coordinated water, the second coordinated water, and structural hydroxyls. A series of Maya blue simulants were prepared by heating the mixture of indigo and sepiolite materials at 180 °C. Reflectance spectroscopy and CIE 1976 color space were employed to characterize color properties and color differences of hybrid pigments. Chemical resistance to concentrated HNO_3 and dimethyl sulfoxide (DMSO), and photostability under visible light were evaluated. Microporous analysis and Fourier transform infrared spectroscopy were applied to study the indigo-sepiolite interaction. Coordinated water was essential for the greenish-blue color and outstanding stability of Maya blue, while zeolitic water and structural hydroxyls did not affect pigments' properties. Indigo molecules were confirmed to be inserted into sepiolite channels and formed hydrogen bonds with coordinated water at one side. Structural hydroxyls were insignificant for the formation of Maya blue. This work provides a guideline for preparing stable clay-dye hybrid pigments.

1. Introduction

Natural dyes and colored minerals are the most widely used colorants in history. For example, Tyrian purple, cochineal red, madder red, and indigo blue were the most important dyeing materials in ancient Europe and Asia [1]. In addition, minerals such as ochre, azurite, lapis lazuli, and malachite were also ground and used as pigments [2]. These colorants not only played a great role in the history of art, but also provided the basis for developing modern high-performance pigments. However, organic dyes are easier to fade, while mineral pigments are more stable. Therefore, pigments that combine organic dyes and inorganic minerals may exhibit fantastic colors and remarkable stability. Indeed, this strategy had been implemented by ancient Maya people as early as more than one thousand years ago. They created a greenish-blue pigment, which was given the name Maya blue. This unique pigment was widely found in Mayan cultural heritages, such as mural paintings, potteries, statues, sacrificial pits, and manuscripts [3–10]. This pigment is resistant to diluted mineral acids, alkalis, solvents, oxidants, reducing agents, moderate heat, and biocorrosion [8,11,12]. Earlier archeologists even declared that the color of Maya blue was not discolored by boiling nitric acid nor by heating much below redness [13,14]. Due to its exceptional color and excellent stability, Maya blue has attracted strong interest from archaeologists and chemists. At the end of the 1950s, palygorskite was confirmed as the component of Maya blue by X-ray diffraction [15]. Later, Van Olphen reported that a Maya blue-like pigment could be prepared by heating the mixture of indigo and palygorskite or sepiolite [16]. After that, indigo was identified as the chromophore of Maya blue by spectroscopic investigations [17,18]. In recent

* Corresponding author. 363, Changxing Road, Tianhe District, Guangzhou, China.
E-mail address: sizhoutufei@163.com (G. Zhuang).

https://doi.org/10.1016/j.dyepig.2022.110138
Received 24 August 2021; Received in revised form 25 December 2021; Accepted 26 January 2022
Available online 30 January 2022

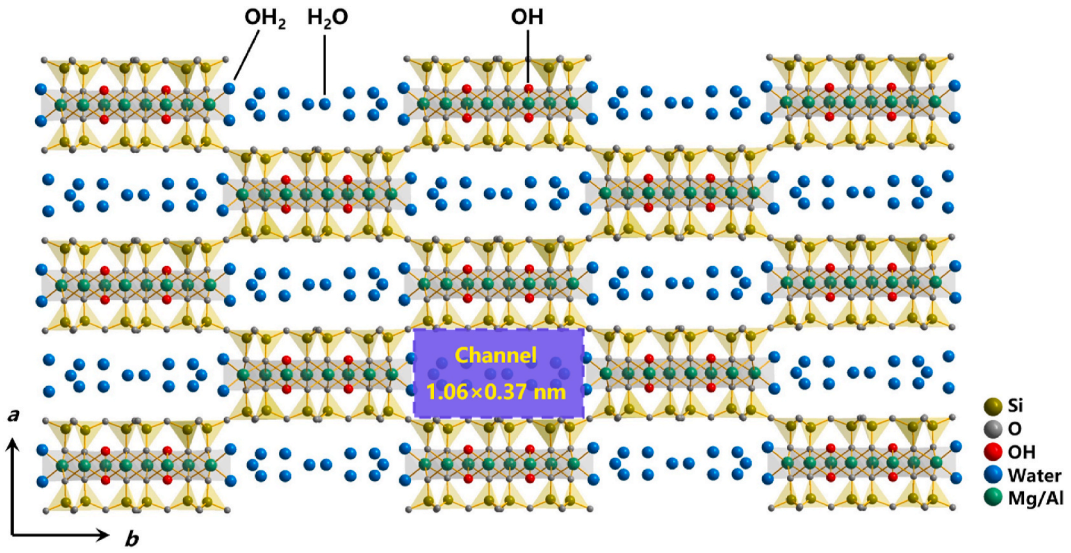

Fig. 1. Structure of sepiolite and different hydroxyl groups (built by Diamond software; H_2O: zeolitic water, OH_2: coordinated water, OH: structural hydroxyl).

two decades, dehydroindigo (oxide compound of indigo) was also considered to contribute to the special color along with indigo according to the electrochemical results [19–25]. Doménech-Carbó et al. (2013) emphasized the presence of dehydroindigo in Maya blue pigment by using pyrolysis–silylation gas chromatography-mass spectrometry (Py–GC–MS) and ultra-pressure liquid chromatography coupled with mass spectrometry (UPLC–MS) [26]. However, vibrational spectroscopic studies did not show evidence of dehydroindigo [27]. Therefore, Maya blue is a hybrid pigment prepared from palygorskite/sepiolite clay minerals and indigo dye, perhaps containing some dehydroindigo. Although the composition of Maya blue has been revealed, the color-causing and stabilization mechanism has not been fully understood. Sepiolite and palygorskite show the following typical features. (i) They contain a TOT structure with two tetrahedral sheets (T) sandwiching an octahedral sheet (O). (ii) Numerous channels (micropores) occur in their structures with the size of 1.06 × 0.37 nm (sepiolite) and 0.64 × 0.37 nm (palygorskite) due to discontinuous octahedral sheets (Fig. 1) [28]. (iii) They have multiple hydroxyl groups, i.e., structural hydroxyls (—OH), coordinated water (OH_2), and zeolitic water (H_2O). According to the structural characteristics of sepiolite and palygorskite, several hypotheses were proposed to explain the formation mechanism of Maya blue. Van Olphen (1966) suggested that indigo molecules are too big to enter the channels of palygorskite and sepiolite [16]. Kleber et al. popularized the idea of indigo molecules being inserted into clay channels [17]. Most studies agreed that dye molecules were inserted into the channels following the release of zeolitic water by heating [29–38]. However, the clay-dye interaction is still unsolved, i.e., some experimental investigations and computational simulations agreed that inserted indigo molecules formed hydrogen bonds with coordinated water [29,31,32,37], while others concurred that indigo molecules directly interacted with octahedral cations [33–35]. Except for inserting into the channels, indigo molecules may stay on the surface and in the surface grooves (open channels). Hubbard et al. (2003) proposed that indigo molecules might be fixed on the clay surface through hydrogen bonds with edge silanol groups, blocking the entrances of channels. Later research agreed that indigo might block the channels, but the hydrogen bonds between indigo and silanol groups were denied. Van Olphen (1966) [16] firstly proposed, and Chiari et al. (2008) [39] agreed that indigo molecules should be easier to enter the surface grooves than to completely occupy channels. Furthermore, the clay-dye interactions in surface grooves were similar to those in channels.

In the past two decades, much work has been carried out in the past two decades to reveal indigo-clay interactions in Maya blue pigment. Manciu et al. (2007) investigated the FT-Raman spectra of synthetic Maya blue at 170 °C for different hours. They found the following three phenomena: (i) the N–H band of indigo disappeared in Maya blue; (ii) the band representing zeolitic water became weak or disappeared; (iii) the C═O band of indigo decreased and finally disappeared in Maya blue, while a new band at 1736 cm^{-1} was assigned to the C═O of dehydroindigo. Accordingly, they proposed that indigo became dehydroindigo, and a bidentate metal might be formed in Maya blue via Al–O and Al–N bonds with dehydroindigo. Tsiantos et al. (2012) reported the near-infrared spectra of Maya blue pigment prepared at different temperatures [27]. Their results suggested that removing zeolitic water and accessibility of channels were prerequisites for the association of indigo with palygorskite, and this association should hinder the rehydration of zeolitic water in Maya blue. The authors suggested that indigo directly bonded with Mg^{2+} because the "coordinated water" would be removed above 150 °C, even above 50 °C in Maya blue. Nevertheless, these authors wrongly analyzed the dehydration process of clay minerals and Mayan blue. Usually, the coordinated water is released at about 300–500 °C, while the mass losses at about 50 and 150 °C are assigned to the dehydration of surface adsorbed water and zeolitic water, respectively [40–42]. Ovarlez et al. [43] investigated the Fourier transform infrared (FT-IR) spectra of indigo-sepiolite hybrid heated at 120–550 °C. They claimed that a blue pigment could be prepared by heating the mixture of sepiolite and indigo at 300–500 °C. They suggested that indigo molecules interacted with octahedral cations, instead of coordinated water, because coordinated water should be removed at 300–550 °C. Similar conclusions were reported in their later work [34]. However, these results are doubtful indigo was not stable above 300 °C, and another work by the same authors reported that heating indigo-sepiolite mixture at 350 °C resulted in a black sample, instead of a blue pigment [44]. Ovarlez et al. (2012) tried to distinguish the influences of different water molecules on indigo-clay interactions by comparing the FT-IR spectra of indigo-clay mixtures and indigo-preheated clay mixtures [44]. The proposed that indigo interacted with clay minerals by hydrogen bonding to coordinated water at lower temperatures, but direct bonding to Mg^{2+} at higher temperatures (280–350 °C). According to the thermal analysis, this hypothesis is not convincing because only half coordinated water was removed at 350 °C. Therefore, indigo molecules might also interact with residual coordinated water. Moreover, there was no evidence of microporous analysis that could verify whether indigo molecules were inserted into the channels. Giustetto et al. [45] argued that indigo should form a hydrogen bond with coordinated water via C═O or N–H, because

thermogravimetry coupled with gas chromatography (TG-GC) results proved that indigo and coordinated water lost simultaneously. They emphasized this hypothesis by investigating the FT-IR, Raman, and NMR results of indigo-sepiolite hybrids [46]. Nevertheless, the simultaneous escape of indigo and coordinated water does not suggest the interaction happened between indigo and coordinated water. Furthermore, the micropore structure of sepiolite before and after forming hybrid pigments was not studied, and no evidence proved the insertion of indigo molecules into the channels.

Although many attempts have been made to unveil the indigo-clay interactions, controversies remain for the following three reasons (i) The roles of hydroxyl groups of clay minerals (i.e., zeolitic water, coordinated water, and structural hydroxyls). in indigo-clay interactions have not been clarified. (ii) Most previous studies focused on the spectroscopic analyses (e.g., FT-IR, Raman, etc.), ignoring the colors, chemical stability, and photostability of pigments. (iii) Microporous analysis, which should be helpful to understand the positions of indigo molecules, was not detailly investigated [40,42].

Therefore, we proposed to study the preparation, color properties, stability, micropore volumes, and FT-IR spectra of hybrid pigments based on heated sepiolite and indigo, aiming to reveal the interaction between indigo and hydroxyl groups and its influence on the physical properties of Maya blue. The raw sepiolite was heated at a certain temperature according to its thermogravimetric results in order to selectively remove zeolitic water, first coordinated, the second coordinated water, and the structural hydroxyls. The reflectance spectra, CIE color parameters, resistance to chemicals and visible light, microporous results, and FT-IR spectra were studied to connect with indigo-hydroxyl interactions.

2. Materials and methods

2.1. Materials

Sepiolite material (marked as Sep) and indigo (97%) were purchased from Shanghai Aladdin Bio-Chem Technology Co., LTD. The XRD pattern of Sep showed typical reflections of sepiolite without any other impurities. Heated sepiolite materials were obtained by two methods. Sep160 were prepared by heating Sep in a vacuum oven (0.1 MPa) at 160 °C for 4 h Sep_{360}, Sep_{610} and Sep_{880} were obtained by heating Sep in a muffle furnace at 360, 610 and 880 °C for 4 h. The final materials were carefully sealed in glass bottles and stored in a desiccator with silica gels to avoid rehydration. Concentrated HNO_3 (68%) and dimethyl sulfoxide (DMSO) were produced by Guangzhou Chemical Reagent Factory.

2.2. Preparation of hybrid pigments

The hybrid pigments were divided into two types, i.e., unheated pigments and heated pigments. An unheated pigment was prepared by mixing sepiolite materials and indigo (2% of the mass of sepiolite materials) in a Fritsch pulveristte 6 type ball mill at the speed of 350 rpm for 3 min. The ball milling method, rather than hand grinding, was employed because ball milling ensured that all the samples were prepared by the same procedure. Unheated pigments were marked as In-Sep_T. Heated pigments were obtained by heating the unheated pigments at 180 °C for 4 h (marked as In-Sep_T-180).

2.3. Characterization

The thermogravimetric (TG) analysis was performed on a NETZSCH STA PC/PG instrument. Approximately 10–20 mg of samples were placed in a platinum crucible on the pan of a microbalance, and then heated from room temperature to 900 °C at a heating rate of 10 °C/min in air. The derivative thermogravimetric (DTG) curves were exported by NETZSCH Proteus software. The BET surface area and micropores measurements were performed on a Micromeritics ASAP-2020 instrument (N_2 adsorption at 77 K). The samples were pre-degassed at 60 °C under vacuum on the apparatus. The degassing process was terminated when the vacuum pressure decreased to 3 μm Hg. FT-IR spectra were collected from a Bruker VERTEX 70v type FT-IR spectrometer in the range of 4000–400 cm^{-1} in vacuum by the potassium bromide pellet technique, with the mass ratio of sample to KBr of 1:100. The final FT-IR spectra, with the resolution of 2 cm^{-1}, were obtained after 64 scans. The UV–Visible absorbance spectra, reflectance spectra, and CIE parameters were obtained from an Ideaoptics (Shanghai) spectrometer FX2000L. The light source of Ideaoptics HL-2000 (wavelength = 380–2000 nm) was used for reflectance spectra and color parameters, while iHL-2000 (wavelength = 250–900 nm) was employed for UV–Visible absorbance spectra. CIE 1976 color space was applied to evaluate the colors of the pigments. Before the reflectance and CIE test, the samples were pressed into tablets slightly by using a 5 mm die set and a metal collar for Quick Press from Tianjin Optical Instrument Factory (HF-2) (see Fig. S1a). All tablets were prepared with 0.02 g sample powder, and the thickness of the tablets was approximately 1 mm. The total color change was calculated as $\Delta E^* = \sqrt{(a_1^* - a_0^*)^2 + (b_1^* - b_0^*)^2 + (L_1^* - L_0^*)}$, where L_1* refers to the L* value of a sample, L_0* refers to the L* value of the reference, and similar to the other two parameters. The digital pictures were obtained by Huawei Mate 20 type mobile phone with three Leica lenses. Photostability was evaluated under visible light for 180 h and 600 h using a CST (Dongguan, China) SL21-63.9-WDG type LED light (Fig. S1c, the emission spectrum can be seen in Fig. S2). The working distance between the light and samples is 10 cm, corresponding to a diameter of 2.5 cm of the working area, with an illuminance of 100 kLux. Hence, the fading test applied for the pigments gave a total light dose of 18000 kLux•h (180 h) and 60000 kLux•h (600 h), being equal to about 30 and 100 years in a common museum gallery illuminated at 200 Lux (10 h of light exposure per day, 6 days per week, and 50 weeks per year). Similar calculations can be found in the literature [47–49]. The light level, i.e., 200 Lux, was selected in this work because the illumination for moderate sensitive artifacts (e.g., oil paintings) was recommended to be 150–200 Lux in a museum [50,51]. The samples for the photostability test were prepared following the procedure of reflectance and CIE tests. Pigments tablets were placed under the light source for illumination (see Fig. S1b). The chemical stability of pigments was assessed by chemical attacks from concentrated HNO_3 (68%) and dimethyl sulfoxide (DMSO). HNO_3 attack was performed as follows: 0.03 g of pigment was added into 2 mL of HNO_3, and the dispersion was shaken for 15 min; then, the dispersion was immediately centrifugated at 6000 rpm and washed three times. DMSO extraction was completed as this procedure: 0.03 g of pigments was added into 5 mL DMSO, shaking for 24 h; the final pigment and corresponding solution were obtained after centrifugation. All the

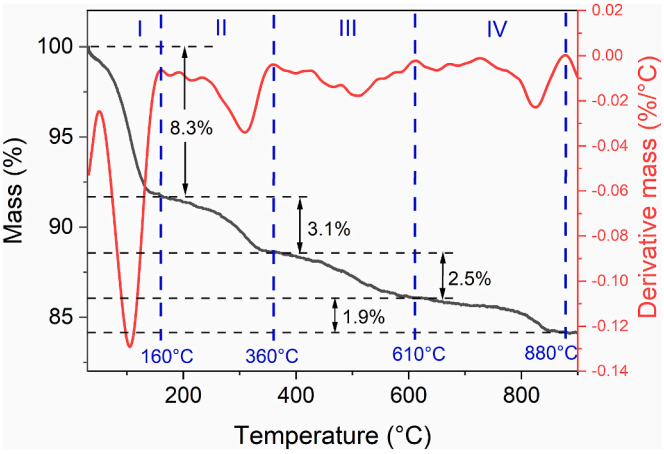

Fig. 2. TG and DTG curves of Sep.

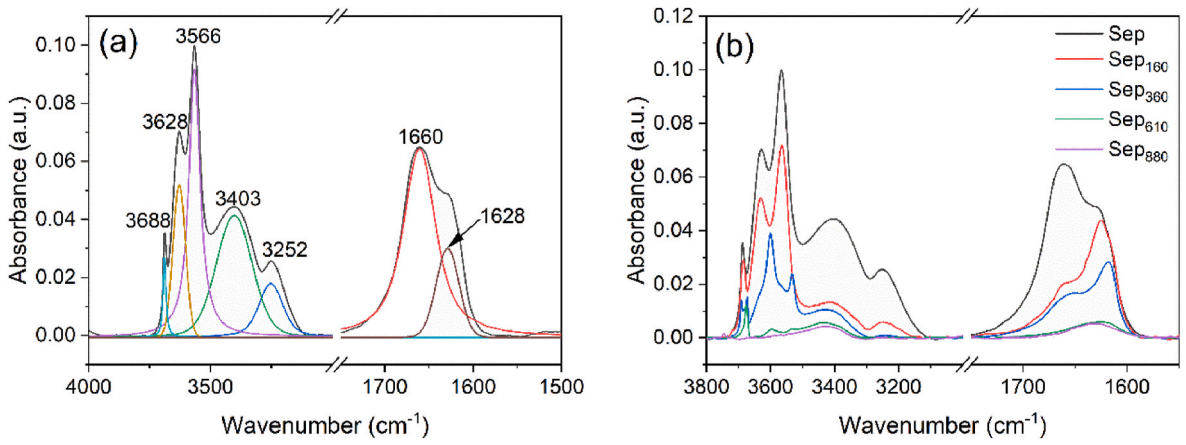

Fig. 3. (a) The FT-IR spectrum of sepiolite and its fitting curves; (b) FT-IR spectra of sepiolite heated at different temperatures.

resulting pigments were dried at 60 °C.

3. Results and discussion

3.1. Structural analysis of sepiolite materials

Four mass loss steps were observed in the TG and DTG curves (Fig. 2) of Sep from room temperature to 900 °C, similar to previous investigations [40,41,52]. Stage I showed a mass loss of 8.3%, corresponding to the release of surface adsorbed water and zeolitic water. Stage II, with a mass loss of 3.1%, is assigned to the removal of the first coordinated water. Stage III, having a mass loss of 2.5%, is attributed to the elimination of the second coordinated water. Finally, stage IV with the minimum mass loss of 1.9% belongs to the dehydroxylation of structural hydroxyls. Stages I to IV ended at about 160, 360, 610, and 880 °C. Therefore, Sep was heated at 160, 360, 610, and 880 °C for 4 h in order to eliminate zeolitic water, the first coordinated water, the second coordinated water, and structural hydroxyls, respectively.

The FT-IR spectra of Sep and heated sepiolite (Fig. 3) confirmed the states of different hydroxyl groups. Usually, the stretching vibrations of hydroxyls appear in the range of 4000–3000 $cm^{-1,}$ while the bending modes of water emerge at 1700-1600 cm^{-1}. Sep presented five distinct bands at 3688, 3628, 3566, 3403, 3252, 1660 and 1628 cm^{-1}, in agreement with previous work [53]. The bands at 3684 corresponded to

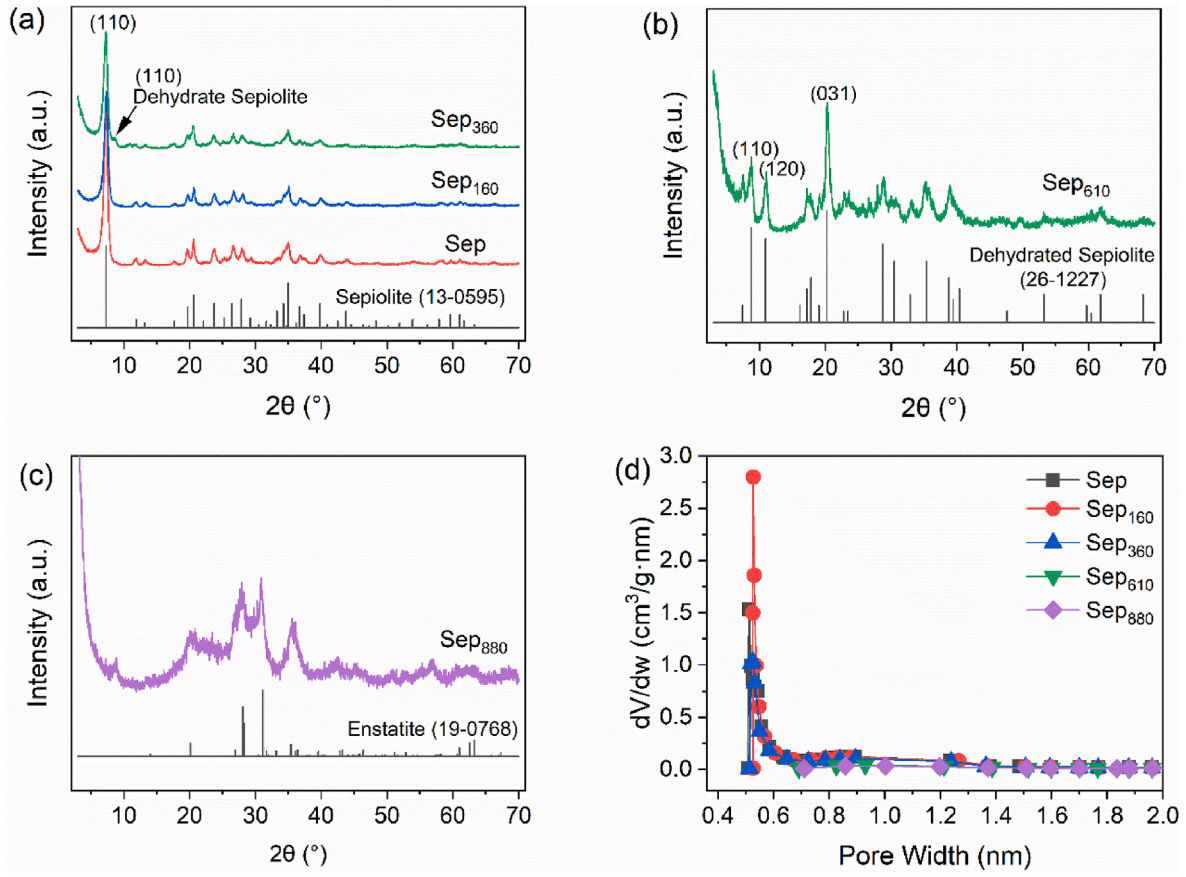

Fig. 4. XRD patterns of (a) Sep, Sep_{160} and Sep_{360}, (b) Sep_{610}, and (c) Sep_{880}; (d) Horvath-Kawazoe differential pore volume versus pore width plots of Sep and heated Sep.

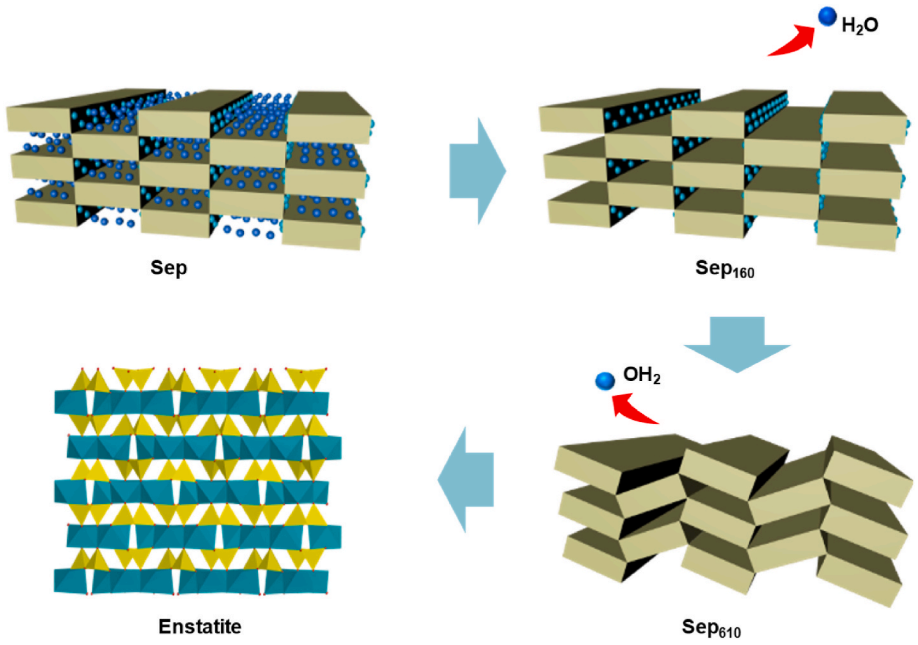

Fig. 5. Schematic diagram of the structural changes of Sep.

the stretching vibrations of Mg_3–OH at trioctahedral sites, while the band at 3628 cm^{-1} belonged to the stretching of Al–Al–OH [54]. The band at 3566 cm^{-1} was mostly assigned to the stretching of coordinated water [52–56], while several reports considered this band as the stretching mode of Fe^{3+}—Fe^{3+}—OH [57–59]. Augsburger suggested that the OH stretching in Al–Mg–OH, Fe–Mg–OH, and Fe_2–OH might contribute to the band at 3566 cm^{-1} because this band was excessively strong and sharp [60]. The wide bands at 3403 and 3252 cm^{-1} are assigned to the stretching mode of zeolitic water and adsorbed water [53,56,61]. The band at 1660 with a shoulder at 1628 cm^{-1} were assigned to the bending vibrations of zeolitic water and coordinated water, respectively [46]. Compared with raw Sep, Sep_{160} exhibited a similar FT-IR spectrum except that the bands of zeolitic water (3403, 3252, and 1660 cm^{-1}) became very weak, indicating that most zeolitic water was lost. The minor bands of zeolitic and adsorbed water were still observed due to little rehydration during the experimental procedure. In the FT-IR spectrum of Sep_{360}, the bands of coordinated water shifted to smaller wavenumbers (3532 and 1618 cm^{-1}) with much lower intensity, indicating the loss of the first coordinated water. Consequently, Mg_3–OH stretching split into two bands (3692 and 3674 cm^{-1}) from 3688, and the stretching of Al–Al–OH shifted to 3600 cm^{-1}. In the FT-IR spectrum of Sep_{610}, the bands of zeolitic water and coordinated water nearly disappeared, while the bands of Mg_3–OH and Al_2–OH remained. In the case of Sep_{880}, all the bands referring to zeolitic water, coordinated water, and hydroxyls vanished. Therefore, ignoring the slight rehydration, sepiolite materials showed different hydroxyl species. Raw Sep contained zeolitic water, coordinated water, and structural hydroxyls. Sep_{160} had coordinated water and structural hydroxyls. Sep_{360} included half coordinated water and structural hydroxyls. Sep_{610} only contained the structural hydroxyls. Finally, Sep_{880} had no hydroxyl species.

The loss of different hydroxyl species should influence the structures of sepiolite materials. As illustrated in Fig. 4a, Sep, Sep_{160}, and Sep_{360} presented a typical XRD pattern of sepiolite with the (110) reflection of sepiolite at $2\theta = 7.32°$ [62]. However, a minor reflection at about $2\theta = 8.75°$, corresponding to dehydrated sepiolite, occurred in the XRD pattern of Sep_{360}. The XRD pattern of Sep_{610} (Fig. 4b) demonstrated that Sep_{610} totally transformed to dehydrated sepiolite, in which the terminal Mg^{2+} complete its coordination with the oxygen of the neighboring silica surface, resulting in structural folding [63,64]. Heated at 880 °C, Sep_{880} became enstatite finally (Fig. 4c) [65,66]. Therefore, the loss of zeolitic water does not influence sepiolite structure, while removing coordinated water and structural hydroxyls resulted in phase change. The status of hydroxyl groups also influenced the surface properties of sepiolite materials (see Table S1). Sep exhibited a narrow micropore volume distribution at 0.51 nm with the maximum dV/dw value of 1.53 $cm^3/g{\cdot}cm$ (Fig. 4d). These micropores were generated by sepiolite channels, as the pore size (0.51 nm) was very close to the channel size (1.06 × 0.37 nm). Sep_{160} and Sep_{360} showed similar micropore volume distribution plots to Sep, but they exhibited different maximum dV/dw values. Compared with the Sep, Sep_{160} had a larger micropore volume while Sep_{360} exhibited a smaller one at 0.51 nm. It is worth noting that pore volume distribution at about 0.51 nm disappeared in Sep_{610} and Sep_{880}. The micropore volume of sepiolite materials increased to the maximum (83.3 mm^3/g) when heated at 160 °C, demonstrating that the removal of zeolitic water resulted in empty channels (Table S1). However, the micropore volumes decreased at higher temperatures. In-Sep_{610} and In-Sep_{880} showed very small micropore volumes, i.e., 6.7 and 1.6 mm^3/g, respectively.

In summary, heating sepiolite at 160, 360, 610, and 880 °C successfully removed zeolitic water, the first coordinated water, the second coordinated water, and structural hydroxyls, respectively. The loss of zeolitic water did not influence the crystal structure but increased the micropore volumes [67]. In the raw Sep, numerous zeolitic water occupied its channels, preventing the entry of nitrogen molecules. The removal of zeolitic water made the channels vacant (Fig. 5). Consequently, the micropore volume of Sep_{160} increased. Although Sep_{360} mostly remained the sepiolite structure, the structural folding started. The structural folding led to the channel size becoming so small that it was difficult to accept nitrogen molecules [41]. Therefore, the micropore volume decreased in Sep_{360} and finally disappeared in Sep_{610}. As Sep_{880} became enstatite, the special structure (see Fig. 5) made no micropores.

3.2. *Influence of the hydroxyl species on colors*

The reflectance spectrum reveals the selective absorption and reflection of visible light. Sepiolite materials showed similar reflectance spectra and high reflectance percentages in the range of 350–800 nm, without any characteristic absorption (Fig. S3). Therefore, the different hydroxyl groups did not obviously influence the reflectance spectra and

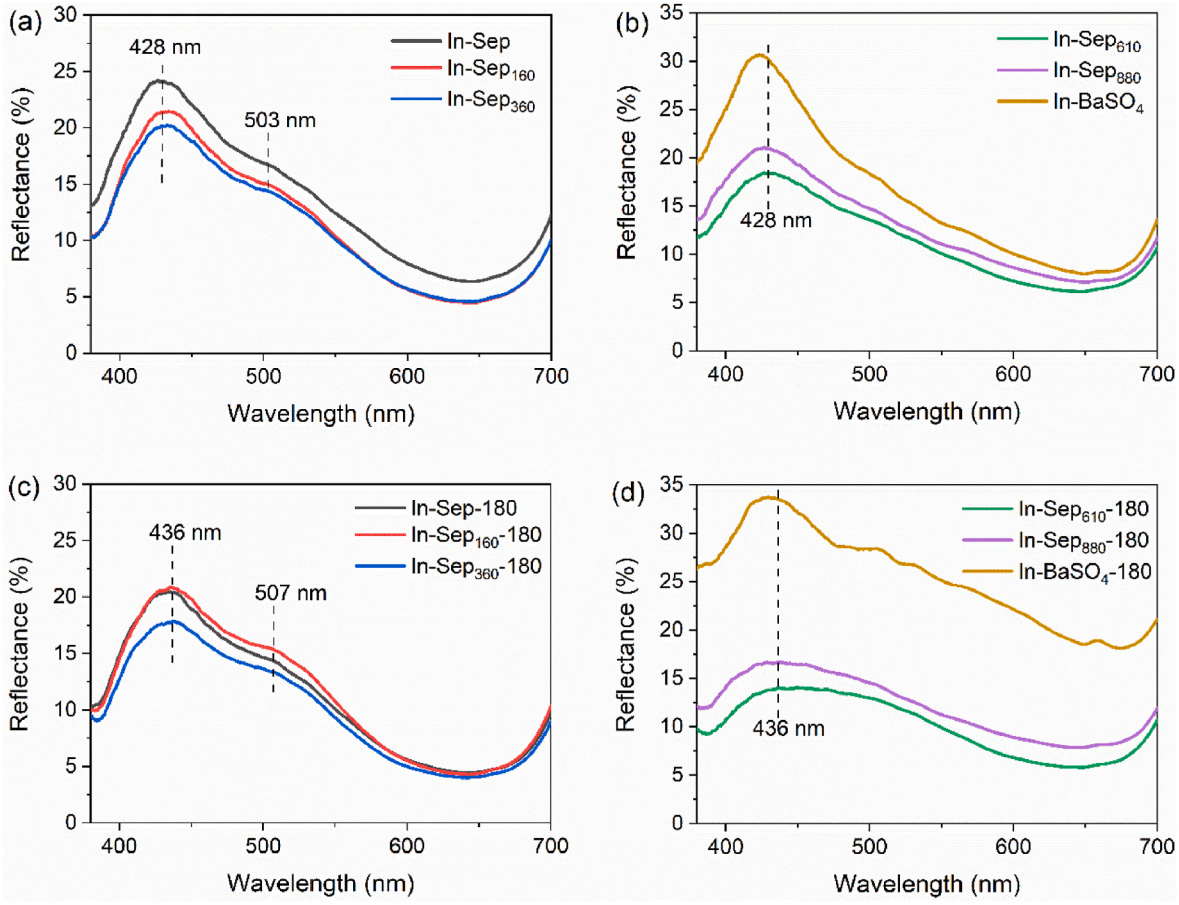

Fig. 6. Reflectance spectra of unheated and heated pigments.

colors of indigo-sepiolite pigments. The reflectance spectrum of pure indigo is also essential to investigate the color nature of pigments. However, pure indigo exhibited extremely low reflectance due to its strong absorption of visible light. It is necessary to mix indigo with inert substrates and prepare similar pigments by the same procedure. Thus, in this work, similar pigments based on indigo and $BaSO_4$ (In–$BaSO_4$ and In–$BaSO_4$-180) were prepared as comparisons.

The reflectance spectra of both unheated pigments (Fig. 6 a and b) are divided into two types depending on whether the pigments contained coordinated water or not. In-Sep, In-Sep_{160}, and In-Sep_{360} (Fig. 6a) showed a prominent reflectance at 428 nm (blue) and a shoulder at 503 nm (green), while In-Sep_{610} and In-Sep_{880} only presented a dominant reflectance at 428 nm without a shoulder (Fig. 6b). The reflectance spectra demonstrated that unheated pigments with coordinated water were blue with little green, while pure blue without coordinated water. The loss of zeolitic water and even the first coordinated water did not significantly influence the reflectance spectra, except for a slight decrease in reflectance percentages. In-Sep_{610} and In-Sep_{880} displayed similar reflectance spectra to In–$BaSO_4$, indicating that indigo did not interact with sepiolite without coordinated water. Like unheated pigments, heated pigments also presented two reflectance spectra depending on coordinated water. Compared with unheated pigments in Fig. 6a, two changes happened in the reflectance spectra of heated pigments in Fig. 6c: (i) the reflectance peaks of heated pigments

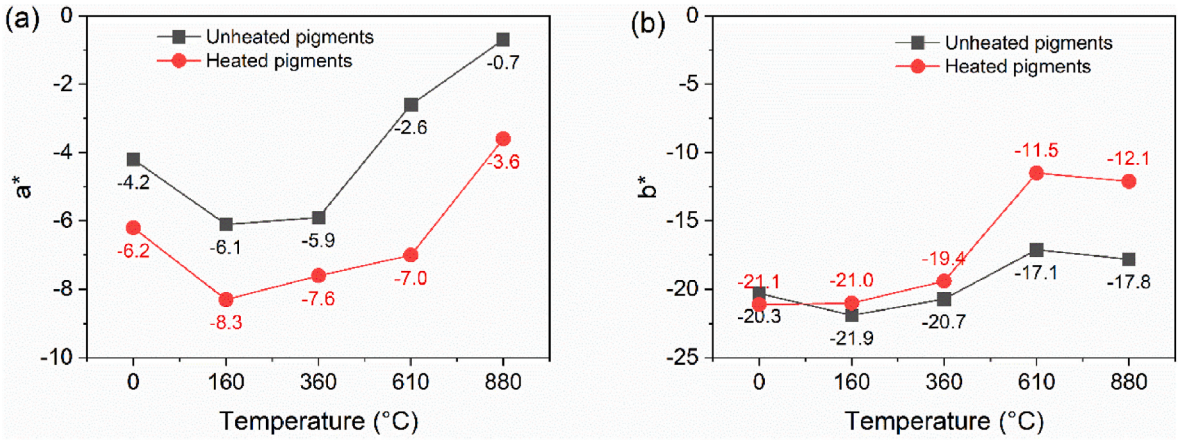

Fig. 7. CIE color parameters of hybrid pigments as a function of pre-heating temperature of Sep.

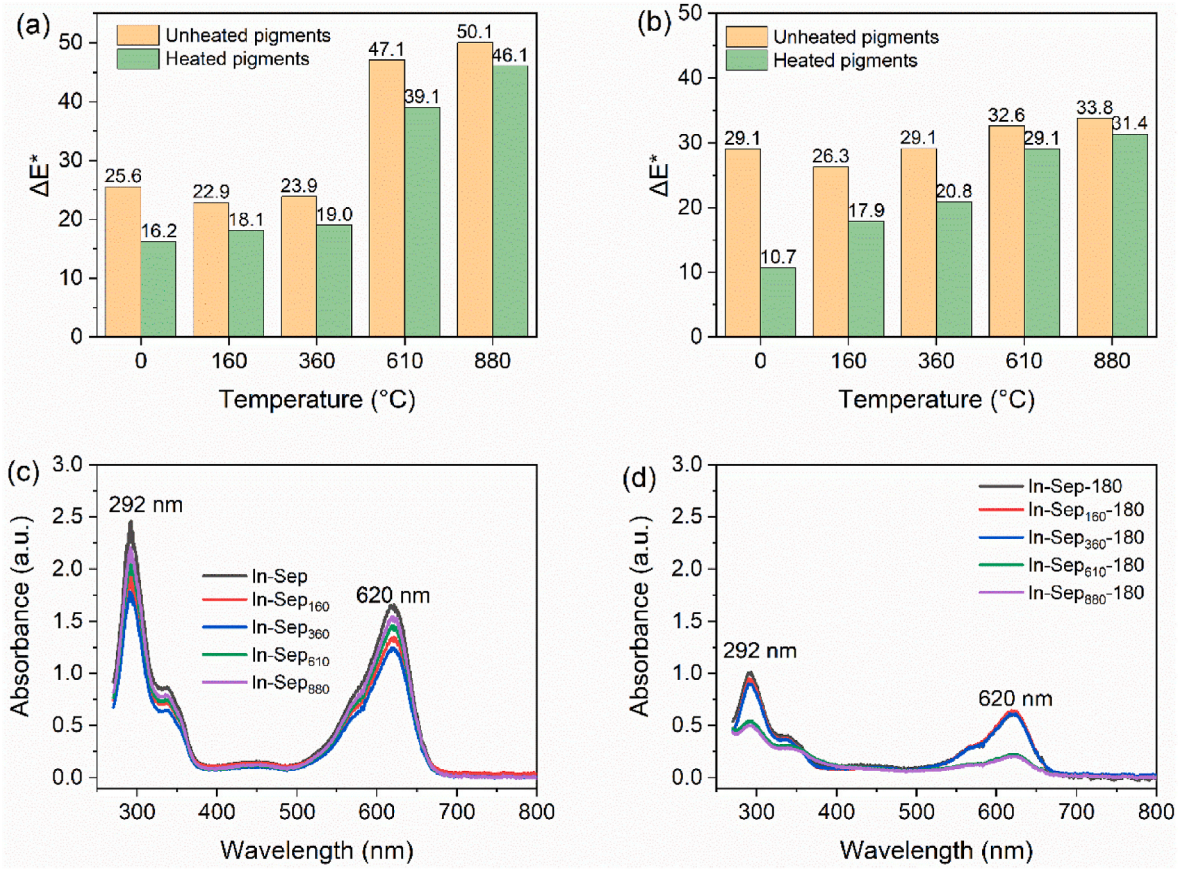

Fig. 8. Color differences of pigments after the attacks of (a) concentrated HNO_3 and (b) DMSO as functions of pre-heating temperatures of sepiolite; UV–visible absorbance spectra of DMSO extracts of (c) unheated and (d) heated pigments.

shifted to a little longer wavelength, i.e., from 428 to 503 nm to 436 and 507 nm, respectively; (ii) the dominant reflectance (436 nm) became weaker while the shoulder (507 nm) became stronger. The similar phenomenon was also reported by Grazia et al. [10]. This phenomenon indicates that thermal treatment made the color of pigments green in the presence of coordinated water. Without coordinated water, In-Sep_{610}-180 and In-Sep_{880}-180 showed similar reflectance spectra to In–$BaSO_4$-180. They exhibited broader and lower reflectance at 400–550 nm than unheated pigments (Fig. 6b), indicating their color fading of pigments without coordinated water.

Besides the reflectance spectra, CIE color parameters can quantitatively reveal the colors of pigments. Like the reflectance spectra results, sepiolite materials showed similar CIE color parameters (Table S2), indicating that hydroxyl groups did not obviously affect the colors of sepiolite materials. All the pigments showed L* values in a narrow range of 35.8–41.2 (Fig. S4). This phenomenon demonstrates that hydroxyl species of sepiolite did not obviously influence the lightness of pigments. Both unheated and heated pigments presented negative a* and b* values, indicating a mixing color of green and blue (Fig. 7). However, the |b*| values were much larger than |a*| values, demonstrating that the pigments' colors were predominantly blue, with minor green. Heated pigments presented larger |a*|values than

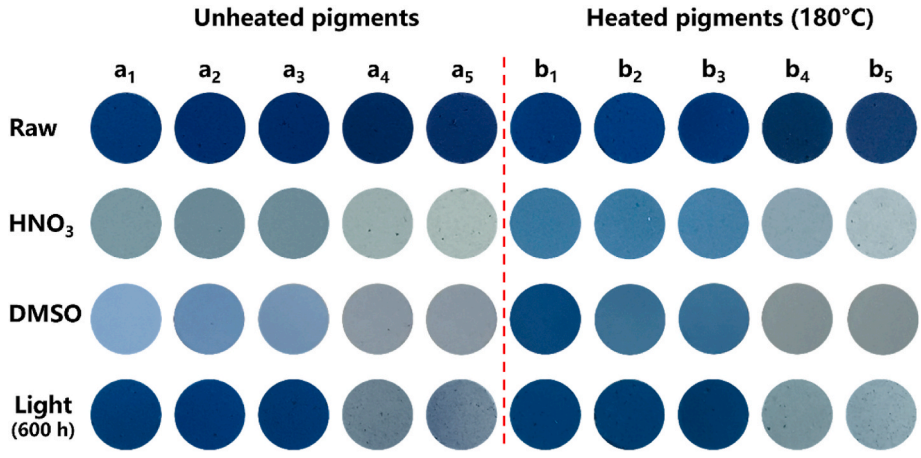

Fig. 9. Digital pictures of hybrid pigments before and after chemical attacks and visible light exposure. a_1 to a_5 refers to In-Sep, In-Sep_{160}, In-Sep_{360}, In-Sep_{610} and In-Sep_{880}; b_1 to b_5 refers to In-Sep-180, In-Sep_{160}-180, In-Sep_{360}-180, In-Sep_{610}-180 and In-Sep_{880}-180 (Detailed CIE color parameters can be seen in Tables S3–8).

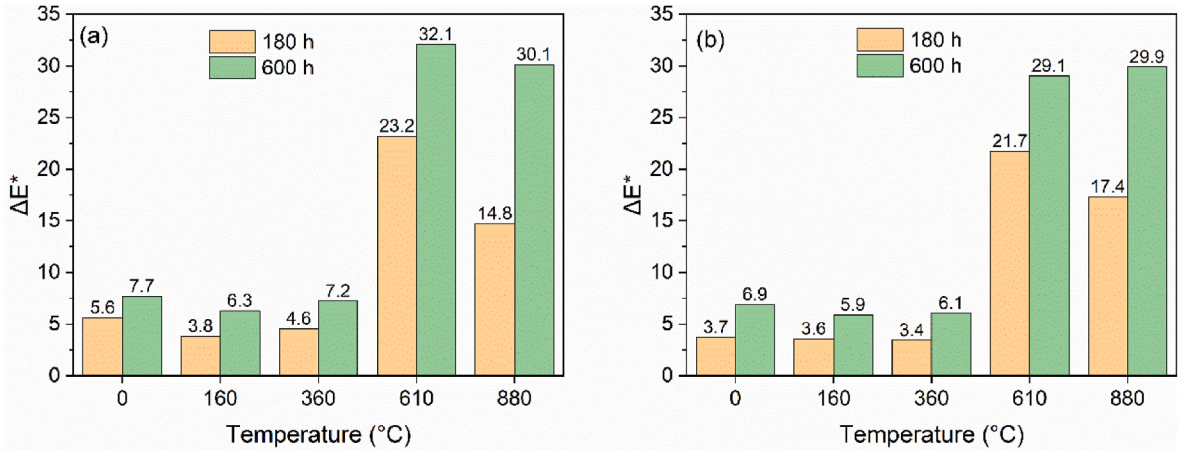

Fig. 10. Color differences of (a) unheated and (b) heated pigments after exposure under visible light for 180 h and 600 h.

unheated pigments, indicating that thermal treatment facilitated the color towards green. The |a*| values increased with the loss of zeolitic water and gradually decreased with the release of coordinated water. When all the hydroxyl species were lost, pigments showed less green hue as the |a*| value was close to zero. Besides, pigments presented similar b* values (19.4–21.9) with coordinated water, while |b*| decreased without coordinated water.

According to the results of reflectance spectra and CIE parameters, the color of indigo-sepiolite hybrid pigments was governed by the hydroxyl species in sepiolite. First, coordinated water is the key to a greenish-blue color. Without coordinated water, a bright greenish-blue pigment cannot be obtained. Second, removing zeolitic water in the channels benefited a green hue. Lastly, structural hydroxyls have no significant influence on the colors of pigments. In conclusion, it is necessary to retain the coordinated water in the sepiolite structure to prepare a greenish-blue pigment.

3.3. Chemical and light resistance of pigments

The color differences of pigments after the attack of concentrated HNO_3 versus the pre-heating temperatures of sepiolite are presented in Fig. 8a. The large ΔE* values of unheated pigments (more than 22) demonstrated considerable color changes after the attack of concentrated HNO_3 (as presented in Fig. 9). However, heated pigments presented a little smaller ΔE* values, indicating that thermal treatment was beneficial to stabilizing indigo-sepiolite pigment. It is worth noting that the ΔE* values varied with the status of coordinated water, i.e., pigments with coordinated water (sepiolite pre-heated below 360 °C) presented smaller ΔE* values than those without coordinated water. For example, In-Sep, In-Sep_{160}, and In-Sep_{360} exhibited ΔE* values of 22.9–25.6 while In-Sep_{610} and In-Sep_{880} showed ΔE* values of 47.1–50.1. A similar phenomenon also happened to heated pigments. These phenomena suggest two meanings: (i) the presence of coordinated water should be essential for the chemical resistance to concentrated HNO_3; (ii) the loss of zeolitic water did not influence the color differences of hybrid pigments. The heated pigment with coordinated water did not completely discolor after the concentrated HNO_3 attack, following the previous reports [13,14,16] on the chemical stability of Maya blue pigment. However, this fact also demonstrates that indigo-sepiolite type Maya blue, is not as stable as claimed by previous researchers because of the significant color differences after the HNO_3 attack.

After DMSO-treatment (Fig. 8b), all the unheated pigments showed similar and large ΔE* values (i.e., in the range of 26.3–33.8), demonstrating significant color changes (see Fig. 9). However, the heated pigments presented different ΔE* values depending on the pre-heating temperature of sepiolite. In-Sep-180 presented the smallest ΔE* value while In-Sep_{880}-180 showed the largest one. According to the thermal analysis results, heating at 160 °C removed all zeolitic water while heating at 180 °C removed a part of coordinated water except for zeolitic water. Therefore, In-Sep-180 contained all the coordinated water while In-Sep_{160}-180 and In-Sep_{360}-180 gradually lost coordinated water. In the case of In-Sep_{610}-180, all the coordinated water was removed. Consequently, the amount of coordinated water molecules is positively related to the chemical resistance to DMSO. The UV–visible absorbance spectra (Fig. 8c and d) of DMSO extracted solutions directly revealed the amount of indigo dissolved into the solvent. The spectra exhibited two dominant absorption peaks at 292 and 620 nm, corresponding to the absorption characteristics of indigo. The extraction of unheated pigments presented similar absorbance spectra, demonstrating that numerous indigo molecules in unheated pigments dissolved into DMSO. However, the extraction solutions of heated pigments exhibited much smaller absorbance than those of unheated pigments. Only a small quantity of indigo molecules was extracted from heated pigments. Hence, heating resulted in the indigo molecules being firmly anchored to sepiolite.

The photostability of a pigment is also essential for its application. Generally, unheated and heated pigments presented similar ΔE* values after visible light exposure for 600 h (Fig. 10), corresponding to being illuminated for more than 100 years in a common museum. Their color differences can be divided into two groups depending on the coordinated water. The first group included pigments in which sepiolite was pre-heated below 360 °C (with coordinated water), while the second group of pigments involved sepiolite that was pre-heated above 610 °C (without coordinated water). Pigments with coordinated water showed the ΔE* values less than 8. However, pigments without coordinated water exhibited ΔE* values up to 32.1. This phenomenon demonstrates that the presence of coordinated water is the key to the light resistance of pigments. In addition, zeolitic water and structural hydroxyls were not significant for photostability. Our previous study proved that similar hybrid pigments based on halloysite (which does not contain coordinated water) exhibited a ΔE* value of more than 12 after 30 years of simulated light exposure [47]. Therefore, coordinated water is significant for the photostability of indigo-clay pigments.

The earliest report about Maya blue's chemical stability was found in Merwin's book chapter [13], where Maya blue was described as a pigment that did not change its color even being treated by boiling nitric acid. However, the concentration of nitric acid was not mentioned. Sánchez del Rio (2006) compared the acid resistance of palygorskite and sepiolite-based Maya blue pigments [68]. They confirmed that Maya blue was resistant to nitric acid (7 mol/L), but longer acid attacks finally resulted in color fading. They also found that sepiolite-based pigment

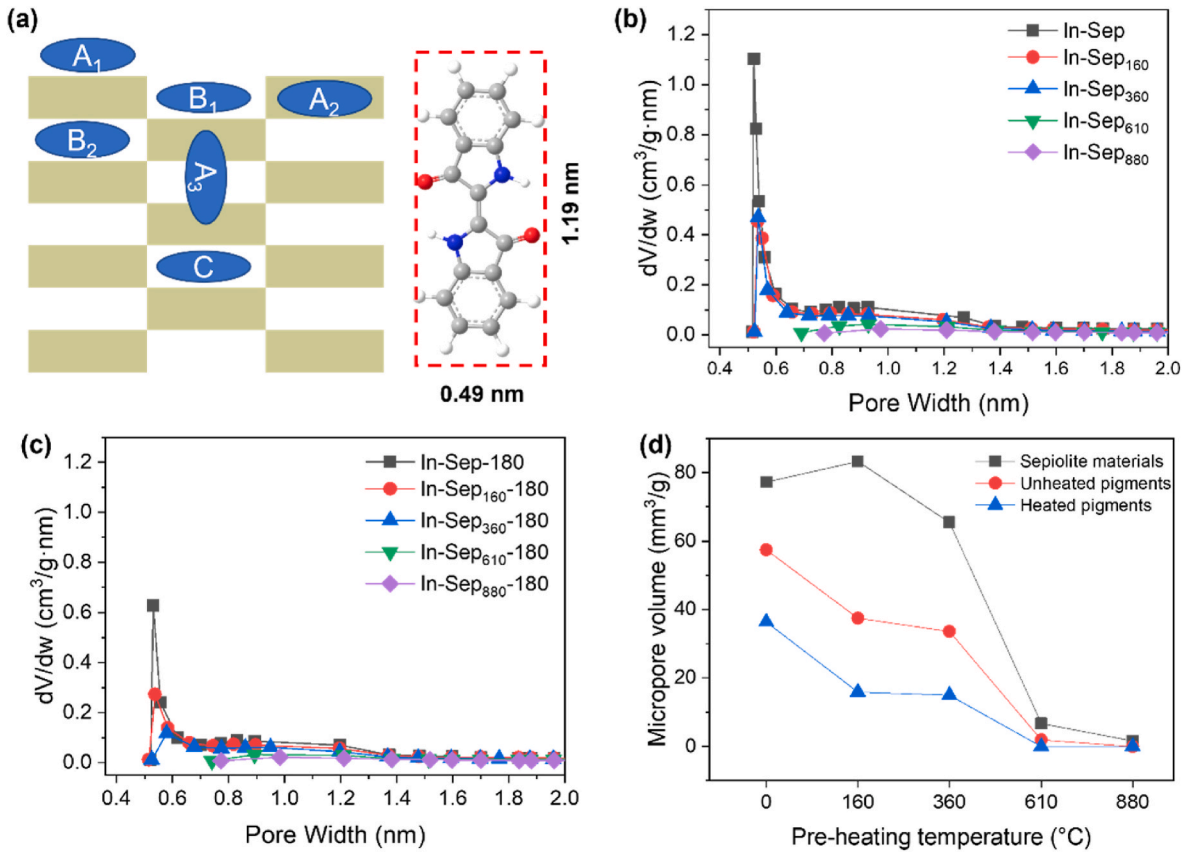

Fig. 11. (a) Possible positions of indigo molecules in the sepiolite structure; Horvath-Kawazoe differential pore volume versus pore width plots of (b) unheated and (c) heated pigments; (d) micropore volumes of sepiolite materials, unheated pigments and heated pigments versus the preheating temperatures.

was less stable than palygorskite pigment. In our study, the ΔE* value of In-Sep-180, In-Sep$_{160}$-180, and In-Sep$_{360}$-180 were in the range of 16.2–19.0, demonstrating a significant color change. But the pigment still displayed a greenish-blue color after the attacks of HNO3 and DMSO (Tables S4 and S6). According to the chemical stability and light resistance results, coordinated water is crucial for stabilizing Maya blue. Opposite phenomena can be found in other indigo-clay hybrid pigments. Neither montmorillonite nor halloysite has coordinated water, so that hybrid pigments based on these two clays and indigo presented awful stability [25,47]. Therefore, the presence of coordinated water contributed to the stabilization of Maya blue.

3.4. Interactions between indigo and sepiolite materials

The color properties, chemical stability, and visible light resistance results of indigo-sepiolite hybrid pigments demonstrated that the properties were highly related to coordinated water. As coordinated water only exists in the channels, the location of indigo molecules is very important for indigo-sepiolite interaction. According to the molecular size of the indigo and the size of channels, indigo molecules have access to the surfaces (positions A_1, A_2, and A_3), open channels (positions B_1 and B_2) and channels (position C) (Fig. 11a). The micropore volumes of hybrid pigments should be sensitive to indigo molecules at different positions. Indigo molecules staying at A_1, A_2, B_1, and B_2 should not significantly influence the micropore volume. However, indigo molecules at position A_3 (covering the entrances) and C (inserting into the channels) should decrease micropore volumes. Therefore, the microporous analysis is helpful for understanding the positions of indigo molecules.

Like sepiolite materials, In-Sep, In-Sep$_{160}$ and In-Sep$_{360}$ presented a sharp pore volume distribution at ca. 0.53 nm (Fig. 11b), while In-Sep$_{610}$ and In-Sep$_{880}$ seldom possessed micropores. Similar micropore volume distributions of heated pigments were plotted in Fig. 11c. This phenomenon indicated that the micropore structure of sepiolite materials remained in the hybrid pigments. However, the micropore volumes (Fig. 11d) of hybrid pigments containing coordinated water were quite different. Compared with Sep, Sep$_{160}$ and Sep$_{360}$, unheated pigments (In-Sep, In-Sep$_{160}$ and In-Sep$_{360}$) presented much smaller micropore volumes, demonstrating that a part of channels was blocked by indigo molecules. In other words, it is definite that indigo molecules stayed at positions A_3 and/or C. Interestingly, Sep$_{160}$ had the largest micropore volume among sepiolite materials, while In-Sep$_{160}$ presented smaller a micropore volume than In-Sep. This phenomenon proved that the micropore volumes of pigments were correlated to water molecules. If indigo molecules only cover the channel entrances (position A_3), the micropore volumes of pigments would be irrelevant to the water molecules in channels. Consequently, it is confirmed that indigo molecules were inserted into the channels (position C), and the loss of zeolitic water made Sep$_{160}$ available to accept more indigo molecules. Importantly, the heated pigments (In-Sep-180, In-Sep$_{160}$-180, and In-Sep$_{360}$-180) exhibited smaller micropore volumes than related unheated pigments, demonstrating heating sepiolite and indigo together resulted in more indigo molecules being inserted into the channels.

Chiari et al. [39] suggested that indigo molecules cannot diffuse throughout palygorskite channels because indigo molecules should block in the entrances. Therefore, they agreed that indigo only stayed in the open channels. Nevertheless, the channel size of sepiolite is much larger than an indigo molecule. Here we confirmed the diffusion of indigo molecules into sepiolite channels by microporous analysis. This result implies that the indigo-sepiolite interaction may be different from the interaction between indigo and palygorskite. The channel size should be considered when discussing the formation of Maya blue

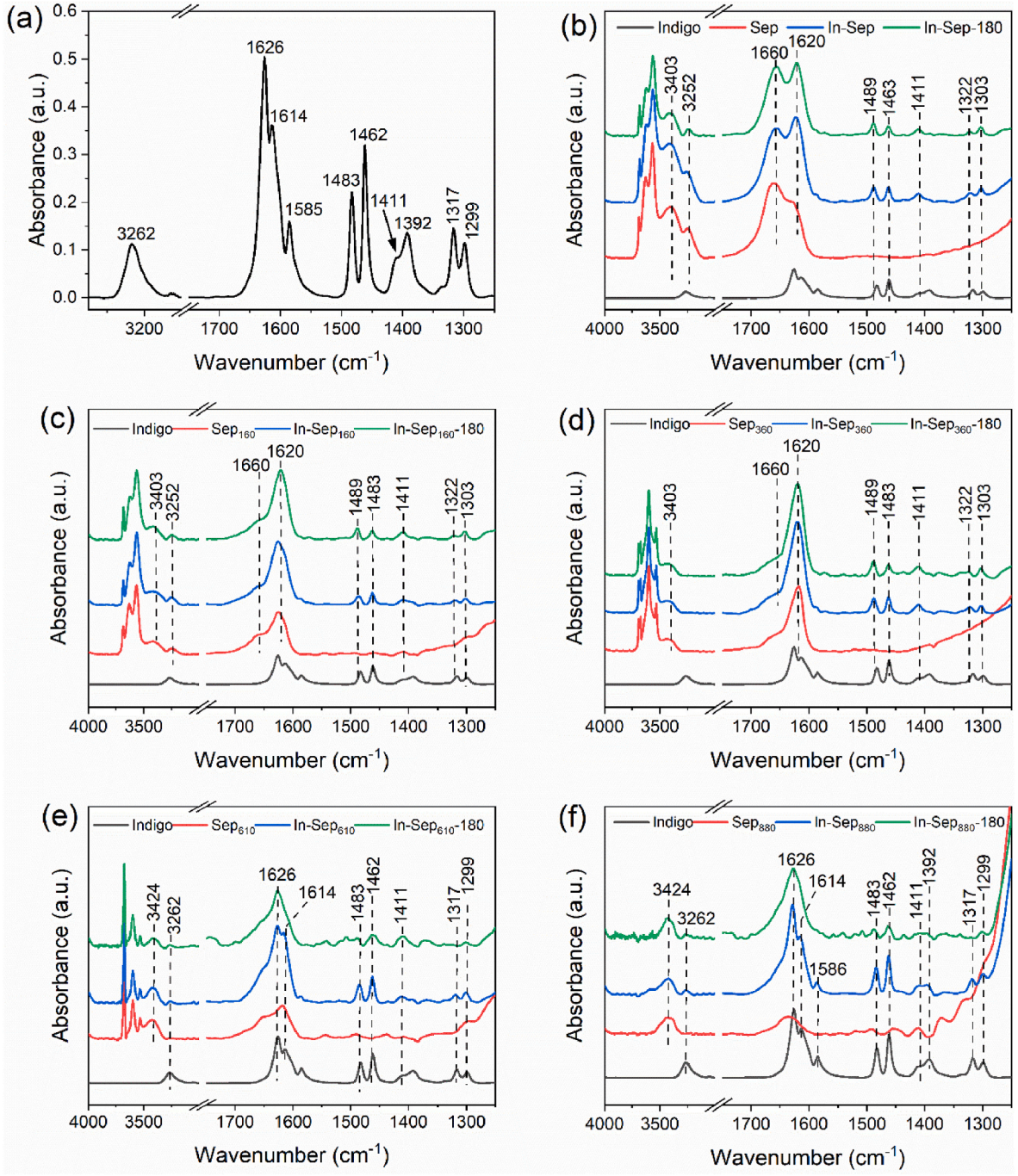

Fig. 12. FT-IR spectra of (a) indigo and (b–f) hybrid pigments.

pigment. Although the insertion of indigo molecules into sepiolite channels was confirmed, indigo molecules could also stay at the surface and open channels (surface grooves). Surface grooves show similar structures and groups (e.g., zeolitic water and coordinated water) to channels. However, since the surface grooves have an open structure, indigo molecules can enter them more easily. Indigo molecules were staying on the surfaces. However, such molecules should not contribute to the special color and remarkable stability of pigments, as pigments without channels presented terrible stability. Therefore, a stable Maya blue-like pigment should ensure that more dye molecules diffuse into the clay channels.

The FT-IR spectra of indigo and hybrid pigments revealed the interaction between sepiolite materials and indigo. As most bands of indigo and sepiolite appear in the range of 4000–1250 cm^{-1}, the FT-IR spectra of pigments were plotted in the range of 4000–1250 cm^{-1}. Indigo showed characteristic bands at 3262, 1626, 1614, 1585, 1483, 1462, 1411, 1392, 1317 and 1299 cm^{-1} (Fig. 12a), similar to previous literature [69,70]. The band at 3262 cm^{-1} was attributed to the stretching of N–H group, while its bending vibration was divided into two bands at 1411 and 1392 cm^{-1}, representing the hydrogen-bonded and free N–H groups [71]. This is because solid indigo is formed by connecting numerous indigo molecules via intermolecular hydrogen bonds [71–73]. The band at 1626 cm^{-1} is attributed to the stretching vibration of C═O. The other bands involve CC and C–H groups [69]. Fig. 12b illustrates the FT-IR spectra of In-Sep and In-Sep-180 compared to Sep. A stronger band at 1620 cm^{-1} appeared while the vibrations of CC and CH groups shifted to larger wavenumbers (1489, 1463, 1322 and 1303 cm^{-1}). Sep showed the bending vibration of coordinated water at

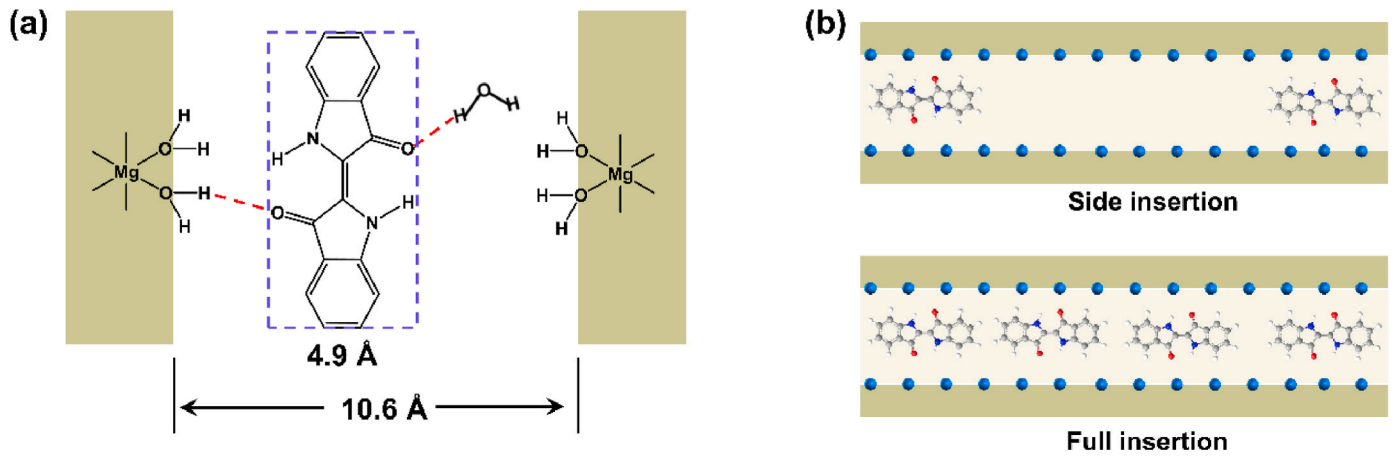

Fig. 13. (a) Schematic diagram of structural changes of indigo; (b) hydrogen bond between indigo and coordinated water.

1628 cm^{-1} with lower intensity than the bending band of zeolitic water. However, the band at 1620 cm^{-1} in pigments was stronger than Sep. Therefore, enhancement of this band was contributed by the stretching of C═O. Bernardino et al. (2016) also confirmed the assignment of C═O at 1620 cm^{-1} in Maya blue by time-resolved infrared spectroscopy [74]. This phenomenon demonstrated that the stretching of C═O shifted to smaller wavenumbers [5]. Similar shifts of C═O were also found in the FT-IR spectra of pigments prepared with Sep_{160} and Sep_{360}, but the spectra of pigment prepared with Sep_{610} and Sep_{880} kept the C═O stretching at 1626 cm^{-1}. This fact demonstrated that the presence of coordinated water significantly influenced the IR bands of C═O and other groups. Except for the shift of C═O stretching, the band of hydrogen-bonded N–H (1392 cm^{-1}) nearly disappeared while the bending vibration of free N–H (1411 cm^{-1}) was enhanced in the presence of coordinated water. The similar IR shift of N–H group was also reported by heating indigo-clay at a moderate temperature [46,75,76]. A reasonable explanation is that the hydrogen bonds between indigo molecules were broken and all the hydrogen-bonded N–H groups transferred into free ones, resulting in the disappearance of hydrogen-bonded N–H groups and the blue-shift of the indigo framework. Accordingly, the IR shift of C═O, CC, CH, and N–H groups happened only in the presence of coordinated water. Without coordinated water, pigments are physical mixtures of sepiolite materials and indigo. Particularly, the bands referring to CC, CH and NH groups became very weak or disappeared in the FT-IR spectra of In-Sep_{610}-180 and In-Sep_{880}-180, indicating that heating caused degradation of indigo in these pigments.

According to the color property, stability, and FT-IR results, we confirmed that coordinated water is crucial for greenish-blue color and remarkable stability of indigo-sepiolite type Maya blue pigment. Theoretically, the breakage of intermolecular hydrogen bonds in indigo will cause the stretching vibration of C═O to move to larger wavenumbers. In contrast, the stretching vibration of C═O shifted to a lower wavenumber instead. A reasonable explanation is that C═O in the indigo molecules formed a new hydrogen bond with palygorskite. In the sepiolite structure, only hydroxyl groups (i.e., zeolitic water, coordinated water and structural hydroxyls) can form hydrogen bonds with C═O, due to their strong polar hydrogen atoms. Zeolite water and structural hydroxyls do not affect the properties and indigo-clay interaction of Maya blue pigment. However, this new hydrogen bond cannot form without coordinated water. Therefore, the hydrogen bonds formed between carbonyls and coordinated water, i.e., C═O … …H–OH, in accordance with most literature [29,31,32,37,45,46,74,77,78]. Several investigations reported that indigo interacted with palygorskite or sepiolite by direct bonding to octahedral cations (Mg^{2+} or Al^{3+}) by C═O after removing coordinated water [33–35]. Nevertheless, coordinated water usually cannot be removed below 200 °C as most Maya blue pigments were prepared at such temperatures. This work confirmed that a Maya blue pigment could not be prepared when the coordinated water in clay minerals was removed. Therefore, indigo molecules should form hydrogen bonds with coordinated water rather than direct bonding to octahedral cations. Usually, the hydrogen bond H … …Y (Y refers to F, O, N, etc.) distance is 160–200 p.m., e.g., the typical length of a hydrogen bond in water is 197 p.m. [79]. The width of a sepiolite channel is 1060 p.m., whereas that of an indigo molecule is about 490 p.m. Therefore, the molecular size of indigo can allow it to form hydrogen bonds with coordinated water at one side [46,80]. In this case, there should be two kinds of C═O groups. i.e., hydrogen-bonded and free ones. However, the FT-IR spectra of pigments presented only one band for C═O at 1620 cm^{-1}. Thus, the residual C═O group might form hydrogen bonds with zeolitic water [45] (Fig. 13a).

The microporous results demonstrated the insertion of indigo molecules into sepiolite channels. Nevertheless, there are two possibilities, i.e., side insertion or full insertion (Fig. 13b). If indigo molecules fully occupied the channels and formed hydrogen bonds with coordinated water, vibrational changes of coordinated water should be observed in the FT-IR spectra of pigments. Unfortunately, the stretching and bending bands of coordinated water in pigments remained the same. Consequently, indigo molecules were probably inserted into the two sides of the channels and formed hydrogen bonds with water molecules. As most coordinated water did not interact with indigo molecules, no shift occurred in the FT-IR spectra. Particularly, indigo molecules were also able to enter the open channels (positions B_1 and B_2 in Fig. 11a). Indeed, indigo molecules were easier to stay at positions B_1 and B_2, due to their open structures. These two positions have the same chemical compositions with internal channels (position C), including the coordinated water. Hence, hydrogen bonds based on indigo and coordinated water also formed at positions B_1 and B_2.

4. Conclusions

A series of indigo-sepiolite hybrid pigments, in which the zeolitic water, coordinated water and structural hydroxyls were selectively removed by thermal treatment, were prepared and characterized. A greenish-blue pigment can only be obtained when coordinated water existed. The chemical stability and photostability of indigo-sepiolite hybrid pigments were also positively related to the coordinated water, whereas zeolitic water and structural hydroxyls seldom influenced the stability of pigments. Thermal treatment at 180 °C facilitated the colors of pigments towards a greenish-blue color. The special hue and remarkable stability of indigo-sepiolite hybrid pigments were contributed by the insertion of indigo molecules into channels of sepiolite and the formation of hydrogen bonds between indigo carbonyls and coordinated water (C═O … …H–OH). An indigo molecule can only form one

hydrogen bond with coordinated water at one side because the channel size is much larger than the width of an indigo molecule. Removing zeolitic water benefited the insertion of indigo molecules into channels. Structural hydroxyls were unavailable to interact with indigo molecules because they were in the internal structure. Therefore, a Maya blue pigment should be prepared by heating the mixture of indigo and clays at an appropriate temperature suitable for removing zeolitic water but does not affect coordinated water. We confirmed that forming hydrogen bonds between clay minerals and organic molecules is an important strategy for the preparation of organic-inorganic nanohybrids. Previous investigations declared that Maya blue-like pigments can only be prepared based on sepiolite and palygorskite minerals. However, by controlling the positions and amount of hydroxyl groups, Maya blue-like pigments may be prepared from other clay minerals and organic dyes. This is significant for developing new clay-based hybrid pigments.

CRediT authorship contribution statement

Li Li: Investigation, Methodology, Writing – original draft. **Guanzheng Zhuang:** Conceptualization, Investigation, Software, Writing – review & editing. **Mengyuan Li:** Investigation, Visualization. **Peng Yuan:** Supervision, Writing – review & editing. **Liangliang Deng:** Writing – review & editing. **Haozhe Guo:** Writing – review & editing.

Declaration of competing interest

The authors declare that they have no known competing financial interests or personal relationships that could have appeared to influence the work reported in this paper.

Acknowledgment

This work is financially supported by Natural Science Foundation of China (No. 4210020241), National Special Support for High-Level Personnel, and Guangdong Basic and Applied Basic Research Foundation (2019A1515110263). This is contribution No.IS-3128 from GIGCAS.

Appendix A. Supplementary data

Supplementary data to this article can be found online at https://doi.org/10.1016/j.dyepig.2022.110138.

References

[1] Volkov VV, Chelli R, Righini R, Perry CC. Indigo chromophores and pigments: structure and dynamics. Dyes Pigments 2020;172:107761.
[2] Siddall R. Mineral pigments in archaeology: their analysis and the range of available materials. Minerals 2018;8(5):201.
[3] José-Yacamán M, Rendón L, Arenas J, Serra Puche MC. Maya blue paint: an ancient nanostructured. Mater Sci 1996;273(5272):223–5.
[4] Ugarte N, Polette LA, Ortega M, Metha A, Wing C, Chianelli RR. In-situ identification of palygorskite in maya blue samples using X-ray powder diffraction. 1998 SSRL activity report: citeseer. 1998.
[5] Leona M, Casadio F, Bacci M, Picollo M. Identification of the pre-columbian pigment mayablue on works of art by noninvasive UV-vis and Raman spectroscopic techniques. J Am Inst Conserv 2004;43(1):39–54.
[6] Sánchez del Río M, Martinetto P, Somogyi A, Reyes-Valerio C, Dooryhee E, Peltier N, et al. Microanalysis study of archaeological mural samples containing Maya blue pigment. Spectrochim Acta B 2004;59(10–11):1619–25.
[7] Vandenabeele P, Bode S, Alonso A, Moens L. Raman spectroscopic analysis of the Maya wall paintings in Ek'Balam, Mexico. Spectrochim Acta A 2005;61(10):2349–56.
[8] Arnold DE, Branden JR, Williams PR, Feinman GM, Brown J. The first direct evidence for the production of Maya Blue: rediscovery of a technology. Antiquity 2008;82(315):151–64.
[9] Vázquez de Ágredos Pascual ML, Doménech Carbó MT, Doménech Carbó A. Characterization of Maya Blue pigment in pre-classic and classic monumental architecture of the ancient pre-Columbian city of Calakmul (Campeche, Mexico). J Cult Herit 2011;12(2):140–8.
[10] Grazia C, Buti D, Amat A, Rosi F, Romani A, Domenici D, et al. Shades of blue: non-invasive spectroscopic investigations of Maya blue pigments. From laboratory mock-ups to Mesoamerican codices. Herit Sci 2020;8(1):1–20.
[11] Reyes-Valerio C. De Bonampak al Templo Mayor: el azul maya en Mesoamérica. Siglo XXI Editores Mexico; 1993.
[12] Sánchez del Río M, Domènech A, Doménech-Carbó MT, Vázquez de Agredos Pascual ML, Suárez M, García-Romero E. The Maya blue pigment. In: Singer A, Galan E, editors. Developments in palygorskite-sepiolite research. Amsterdam, The Netherlands: Elsevier; 2011. p. 453–81.
[13] Merwin HE. Chemical analysis of pigments. In: Morris EH, Charlot J, Morris AA, editors. Temple of the warriors at Chitchen-Itza, Yucatan. Washington DC: Carnegie Institution of Washington; 1931. p. 355–6.
[14] Gettens RJ, Stout GL. Painting materials: a short encyclopaedia. New York: Van Nostrand; 1942.
[15] Gettens RJ. Maya blue: an unsolved problem in ancient pigments. Am Antiq 1962;27(4):557–64.
[16] Van Olphen H. Maya blue: a clay-organic pigment? Science 1966;154(3749):645–6.
[17] Kleber R, Masschelein-kleiner L, Thissen J. Étude et Identification du 'Bleu Maya'. Stud Conserv 1967;12(2):41–56.
[18] Witke K, Brzezinka KW, Lamprecht I. Is the indigo molecule perturbed in planarity by matrices? J Mol Struct 2003;661(661):235–8.
[19] Doménech A, Doménech-Carbó MT, Vázquez de Agredos Pascual ML. Indigo/dehydroindigo/palygorskite complex in maya blue: an electrochemical approach. J Phys Chem C 2007;111(12):4585–95.
[20] Doménech A, Doménech-Carbó MT, Vázquez de Agredos Pascual ML. Dehydroindigo:A new piece into the maya blue puzzle from the voltammetry of microparticles approach. J Phys Chem B 2006;110(12):6027–39.
[21] Doménech-Carbó A, Holmwood S, Di Turo F, Montoya N, Valle-Algarra FM, Edwards HG, et al. Composition and color of maya blue: reexamination of literature data based on the dehydroindigo model. J Phys Chem C 2019;123(1):770–82.
[22] Rondao R, de Melo JSS, Bonifacio VDB, Melo MJ. Dehydroindigo, the forgotten indigo and its contribution to the color of maya blue. J Phys Chem A 2010;114(4):1699–708.
[23] Domenech A, Domenech-Carbo MT, del Rio MS, Pascual MLVD. Comparative study of different indigo-clay Maya Blue-like systems using the voltammetry of microparticles approach. J Solid State Electrochem 2009;13(6):869–78.
[24] Doménech A, Doménech-Carbó MaT, Sanchez del Rio M, Vázquez de Agredos Pascual ML, Lima E. Maya Blue as a nanostructured polyfunctional hybrid organic-inorganic material: the need to change paradigms. New J Chem 2009;33(12):2371–9.
[25] Doménech A, Doménech-Carbó MaT, Sanchez del Rio M, Goberna S, Lima E. Evidence of topological indigo/dehydroindigo isomers in Maya blue-like complexes prepared from palygorskite and sepiolite. J Phys Chem C 2009;113(28):12118–31.
[26] Domenech-Carbo A, Domenech-Carbo MT, Valle-Algarra FM, Domine ME, Osete-Cortina L. On the dehydroindigo contribution to Maya Blue. J Mater Sci 2013;48(20):7171–83.
[27] Tsiantos C, Tsampodimou M, Kacandes GH, del Rio MS, Gionis V, Chryssikos GD. Vibrational investigation of indigo-palygorskite association(s) in synthetic Maya blue. J Mater Sci 2012;47(7):3415–28.
[28] Guggenheim S, Krekeler MPS. The structures and microtextures of the palygorskite–sepiolite group minerals. In: Galàn E, Singer A, editors. Developments in clay science. Elsevier; 2011. p. 3–32.
[29] Chiari G, Giustetto R, Ricchiardi G. Crystal structure refinements of palygorskite and Maya Blue from molecular modelling and powder synchrotron diffraction. Eur J Mineral 2003;15(1):21–33.
[30] Fois E, Gamba A, Tilocca A. On the unusual stability of Maya blue paint: molecular dynamics simulations. Microporous Mesoporous Mater 2003;57(3):263–72.
[31] Reinen D, Kohl P, Muller C. The nature of the colour centres in 'Maya blue' - the incorporation of organic pigment molecules into the palygorskite lattice. Z Anorg Allg Chem 2004;630(1):97–103.
[32] Giustetto R, Levy D, Chiari G. Crystal structure refinement of Maya Blue pigment prepared with deuterated indigo, using neutron powder diffraction. Eur J Mineral 2006;18(5):629–40.
[33] Fuentes ME, Pena B, Contreras C, Montero AL, Chianelli R, Alvarado M, et al. Quantum mechanical model for maya blue. Int J Quant Chem 2008;108(10):1664–73.
[34] Ovarlez S, Giulieri F, Chaze AM, Delamare F, Raya J, Hirschinger J. The incorporation of indigo molecules in sepiolite tunnels. Chemistry-Eur J 2009;15(42):11326–32.
[35] Tilocca A, Fois E. The color and stability of maya blue: TDDFT calculations. J Phys Chem C 2009;113(20):8683–7.
[36] Dejoie C, Martinetto P, Dooryhée E, Brown R, Blanc S, Bordat P, et al. Diffusion of indigo molecules inside the palygorskite clay channels. MRS Proceedings 2011;1319.
[37] Bernardino ND, Constantino VRL, de Faria DLA. Probing the indigo molecule in maya blue simulants with resonance Raman spectroscopy. J Phys Chem C 2018;122(21):11505–15.
[38] Caliandro R, Toson V, Palin L, Conterosito E, Aceto M, Gianotti V, et al. New hints on the maya blue formation process by PCA-assisted in situ XRPD/PDF and optical spectroscopy. Chem Eur J 2019;25(49):11503–11.
[39] Chiari G, Giustetto R, Druzik J, Doehne E, Ricchiardi G. Pre-columbian nanotechnology: reconciling the mysteries of the maya blue pigment. Appl Phys A 2008;90(1):3–7.

[40] Frost RL, Ding Z. Controlled rate thermal analysis and differential scanning calorimetry of sepiolites and palygorskites. Thermochim Acta 2003;397(1–2):119–28.
[41] Kuang WX, Facey GA, Detellier C. Dehydration and rehydration of palygorskite and the influence of water on the nanopores. Clay Clay Miner 2004;52(5):635–42.
[42] Álvarez A, Santarén J, Esteban-Cubillo A, Aparicio P. Chapter 12 - current industrial applications of palygorskite and sepiolite. In: Galàn E, Singer A, editors. Developments in clay science. Elsevier; 2011. p. 281–98.
[43] Ovarlez S, Chaze A-M, Giulieri F, Delamare F. Indigo chemisorption in sepiolite. Application to Maya blue formation. Compt Rendus Chem 2006;9(10):1243–8.
[44] Ovarlez S, Giulieri F, Delamare F, Sbirrazzuoli N, Chaze AM. Indigo-sepiolite nanohybrids: temperature-dependent synthesis of two complexes and comparison with indigo-palygorskite systems. Microporous Mesoporous Mater 2011;142(1):371–80.
[45] Giustetto R, Wahyudi O, Corazzari I, Turci F. Chemical stability and dehydration behavior of a sepiolite/indigo Maya Blue pigment. Appl Clay Sci 2011;52(1–2):41–50.
[46] Giustetto R, Seenivasan K, Bonino F, Ricchiardi G, Bordiga S, Chierotti MR, et al. Host/guest interactions in a sepiolite-based maya blue pigment: a spectroscopic study. J Phys Chem C 2011;115(34):16764–76.
[47] Zhuang G, Jaber M, Rodrigues F, Rigaud B, Walter P, Zhang Z. A new durable pigment with hydrophobic surface based on natural nanotubes and indigo: interactions and stability. J Colloid Interface Sci 2019;552:204–17.
[48] Zhuang G, Rodrigues F, Zhang Z, Fonseca MG, Walter P, Jaber M. Dressing protective clothing: stabilizing alizarin/halloysite hybrid pigment and beyond. Dyes Pigments 2019;166:32–41.
[49] Guillermin D, Debroise T, Trigueiro P, de Viguerie L, Rigaud B, Morlet-Savary F, et al. New pigments based on carminic acid and smectites: a molecular investigation. Dyes Pigments 2018;160:971–82.
[50] Cannon-Brookes S. Daylighting museum galleries: a review of performance criteria. Int J Light Res Technol 2000;32(3):161–8.
[51] Sharif-Askari H, Abu-Hijleh B. Review of museums' indoor environment conditions studies and guidelines and their impact on the museums' artifacts and energy consumption. Build Environ 2018;143:186–95.
[52] Khorami J, Lemieux A. Comparison of attapulgites from different sources using TG/DTG and FTIR. Thermochim Acta 1989;138(1):97–105.
[53] Frost RL, Locos OB, Ruan H, Kloprogge JT. Near-infrared and mid-infrared spectroscopic study of sepiolites and palygorskites. Vib Spectrosc 2001;27(1):1–13.
[54] Suárez M, Garcia E. FTIR spectroscopic study of palygorskite: influence of the composition of the octahedral sheet. Appl Clay Sci 2006;31(1–2):154–63.
[55] Yan W, Liu D, Tan D, Yuan P, Chen M. FTIR spectroscopy study of the structure changes of palygorskite under heating. Spectrochim Acta A 2012;97(1):1052–7.
[56] Frost RL, Cash GA, Kloprogge JT. 'Rocky Mountain leather', sepiolite and attapulgite - an infrared emission spectroscopic study. Vib Spectrosc 1998;16(2):173–84.
[57] Chahi A, Petit S, Decarreau A. Infrared evidence of dioctahedral-trioctahedral site occupancy in palygorskite. Clay Clay Miner 2002;50(3):306–13.
[58] Gionis V, Kacandes GH, Kastritis ID, Chryssikos GD. On the structure of palygorskite by mid- and near-infrared spectroscopy. Am Mineral 2006;91(7):1125–33.
[59] Besson G, Drits VA. Refined relationships between chemical composition of dioctahedral fine-grained mica minerals and their infrared spectra within the OH stretching region. Part I: identification of the OH stretching bands. Clay Clay Miner 1997;45(2):158–69.
[60] Augsburger M. FTIR and Mssbauer investigation of a substituted palygorskite : silicate with a channel structure. J Phys Chem Solid 1998;59(2):175–80.
[61] Cheng H, Yang J, Frost RL, Wu Z. Infrared transmission and emission spectroscopic study of selected Chinese palygorskites. Spectrochim Acta Mol Biomol Spectrosc 2011;83(1):518–24.
[62] Suárez M, García-Rivas J, García-Romero E, Jara N. Mineralogical characterisation and surface properties of sepiolite from Polatli (Turkey). Appl Clay Sci 2016;131:124–30.
[63] Preisinger A. Sepiolite and related compounds: its stability and application. Clay Clay Miner 1961;10:365–71.
[64] Serratosa JM. Surface properties of fibrous clay minerals (palygorskite and sepiolite). In: Mortland MM, Farmer VC, editors. International Clay Conference 1978, Proceedings of the VI International Clay Conference 1978, organized by the Clay Minerals Group, Mineralogical Society, London, under the auspices of Association Internationale pour l'Etude des Argiles. Elsevier; 1979. p. 99–109.
[65] Yener N, Önal M, Üstünışık G, Sarıkaya Y. Thermal behavior of a mineral mixture of sepiolite and dolomite. J Therm Anal Calorim 2007;88(3):813–7.
[66] Yilmaz MS, Kalpakli Y, Piskin S. Thermal behavior and dehydroxylation kinetics of naturally occurring sepiolite and bentonite. J Therm Anal Calorim 2013;114(3):1191–9.
[67] Kuang W, Facey GA, Detellier C, Casal B, Serratosa JM, Ruiz-Hitzky E. Nanostructured hybrid materials formed by sequestration of pyridine molecules in the tunnels of sepiolite. Chem Mater 2003;15(26):4956–67.
[68] Sánchez del Rio M, Martinetto P, Reyes-Valerio C, Dooryhee E, Suárez M. Synthesis and acid resistance of Maya Blue pigment. Archaeometry 2006;48(1):115–30.
[69] Tatsch E, Schrader B. Near-infrared fourier transform Raman spectroscopy of indigoids. J Raman Spectrosc 1995;26(6):467–73.
[70] Amat A, Rosi F, Miliani C, Sgamellotti A, Fantacci S. Theoretical and experimental investigation on the spectroscopic properties of indigo dye. J Mol Struct 2011;993(1–3):43–51.
[71] Weinstein J, Wyman GM. Spectroscopic studies on dyes. i. the association of indigo dyes in the solid phase1. J Am Chem Soc 1956;78(11):2387–90.
[72] Monahan AR, Kuder JE. Spectroscopic differences between crystalline and amorphous phases of indigo. J Org Chem 1972;37(25):4182–4.
[73] Süsse P, Steins M, Kupcik V. Indigo - crystal-structure refinement based on synchrotron data. Z Kristallogr 1988;184(3–4):269–73.
[74] Bernardino ND, Brown-Xu S, Gustafson TL, de Faria DLA. Time-resolved spectroscopy of indigo and of a maya blue simulant. J Phys Chem C 2016;120(38):21905–14.
[75] Manciu FS, Reza L, Polette LA, Torres B, Chianelli RR. Raman and infrared studies of synthetic Maya pigments as a function of heating time and dye concentration. J Raman Spectrosc 2007;38(9):1193–8.
[76] Sánchez del Río M, Boccaleri E, Milanesio M, Croce G, van Beek W, Tsiantos C, et al. A combined synchrotron powder diffraction and vibrational study of the thermal treatment of palygorskite-indigo to produce Maya blue. J Mater Sci 2009;44(20):5524–36.
[77] Sánchez-Ochoa F, Cocoletzi GH, Canto G. Trapping and diffusion of organic dyes inside of palygorskite clay: the ancient Maya Blue pigment. Microporous Mesoporous Mater 2017;249:111–7.
[78] Raya J, Hirschinger J, Ovarlez S, Giulieri F, Chaze A-M, Delamare F. Insertion of indigo molecules in the sepiolite structure as evidenced by ^{1}H–^{29}Si heteronuclear correlation spectroscopy. Phys Chem Chem Phys 2010;12(43):14508–14.
[79] Legon AC, Millen DJ. Angular geometries and other properties of hydrogen-bonded dimers: a simple electrostatic interpretation of the success of the electron-pair model. Chem Soc Rev 1987;16:467–98. 0.
[80] Giustetto R, Seenivasan K, Bordiga S. Spectroscopic characterization of a sepiolite-based Maya Blue pigment. Period Mineral 2010;59:21–37.